

1969

## Exponential analysis of arterial pressure waves

Lawrence M. Rice  
*University of Nebraska Medical Center*

This manuscript is historical in nature and may not reflect current medical research and practice. Search [PubMed](#) for current research.

Follow this and additional works at: <https://digitalcommons.unmc.edu/mdtheses>



Part of the [Medical Education Commons](#)

---

### Recommended Citation

Rice, Lawrence M., "Exponential analysis of arterial pressure waves" (1969). *MD Theses*. 121.  
<https://digitalcommons.unmc.edu/mdtheses/121>

This Thesis is brought to you for free and open access by the Special Collections at DigitalCommons@UNMC. It has been accepted for inclusion in MD Theses by an authorized administrator of DigitalCommons@UNMC. For more information, please contact [digitalcommons@unmc.edu](mailto:digitalcommons@unmc.edu).

EXponential ANALYSIS OF  
ARTERIAL PRESSURE WAVES

by

LAWRENCE M. RICE, B.S.

A THESIS

Presented to the Faculty of  
The Graduate College in the University of Nebraska

In Partial Fulfillment of Requirements  
For the Degree of Master of Science  
Department of Electrical Engineering

Under the Supervision of  
Grant G. Myers, B.S., M.S., Ph.D.

Lincoln, Nebraska

January 1968

*Class of 1969*

## ACKNOWLEDGEMENT

The author wishes to sincerely express his appreciation to his professor, Dr. Grant G. Myers, thesis advisor, and Charles R. Goetowski, who both unselfishly expended much time and effort helping to prepare this thesis.

513554

## ABSTRACT

The damped exponential approach to signal representation was first introduced by Huggins. This paper utilizes this approach in the analysis of the descending limb of the peripheral arterial pressure wave. Since these waveforms are similar to damped exponentials, the important attributes of the signal can be conveniently measured.

TABLE OF CONTENTS

I. ACKNOWLEDGEMENT ..... ii

II. ABSTRACT ..... iii

III. INTRODUCTION ..... 1

IV. PHILOSOPHY OF SIGNAL ANALYSIS ..... 2

V. SIGNAL REPRESENTATION BY DAMPED EXPONENTIALS ..... 4

VI. THE PROBLEM OF SELECTING A BASIS SET ..... 5

VII. CONSTRUCTION OF AN ORTHONORMAL  
SET OF FUNCTIONS ..... 7

VIII. DETERMINATION OF THE SIGNAL COORDINATES ..... 9

IX. EXPERIMENTAL SELECTION OF  
COMPONENT EXPONENTIALS ..... 10

X. CONSTRUCTION OF THE EXPERIMENTAL SET  
OF ORTHONORMAL FUNCTIONS ..... 11

XI. DATA AND METHODS ..... 13

XII. RESULTS AND DISCUSSION ..... 15

XIII. SUMMARY OF RESULTS ..... 17

XIV. SUGGESTIONS FOR FURTHER STUDY ..... 17

XV. APPENDIX ..... 18

XVI. BIBLIOGRAPHY ..... 42

## INTRODUCTION

The waveform of the arterial pulse has long been of medical-physiological interest. When palpating the radial pulse, clinicians subjectively attempt to ascertain the contour of the pulsation. Certain types of pulses are known to be associated with disease. For instance a bounding or collapsing pulse is encountered in hypertension, emotional states and aortic regurgitation (1). A pulse which has a prolonged upstroke and a blunted peak is associated with severe degrees of aortic stenosis.

With the advent of arterial catheterization techniques it has been possible to record pressure waveforms in both central as well as peripheral arteries. Central pressure waveforms found in a number of clinical conditions as described by Wiggers (2) are shown in Figure 1.

Attempts to categorize waveforms objectively have led to both time domain and frequency domain analyses. Most time domain studies have emphasized some parameter of the waveform such as its derivative. For example, Mason (3) claims that analysis of the first and second derivatives of the brachial pressure curve is helpful in the differentiation of valvular aortic stenosis, combined stenosis and regurgitation, and pure aortic regurgitation. In a recent study by Arani and Charleton (4) it was found that the derivative of the rising pressure curve was correlated

with the degree of aortic stenosis when an estimate of arterial compliance was taken into account. Simmons (5) has written a computer program to analyze selected samples of the peripheral pulse wave in order to obtain information about the normal range of pulse wave variations.

Frequency domain analysis was employed by Puls and Heizer (6) who performed Fourier transforms on peripheral pulse waves of patients grouped by age. They noted that in general the "d-c" component of the waveform was decreased in older age groups, presumably reflecting the higher incidence of arteriosclerosis in these groups. Goldwyn and Watt (7) have attempted to characterize the descending portion of the arterial waveform by parameters of a circuit model which they have developed. Their approach will be presented in a later section. An exponential approach to the analysis of the pulse waveform has not been found in the literature.

#### PHILOSOPHY OF SIGNAL ANALYSIS

Huggins (8,9) remarks that signal representations are needed for either of two purposes: to represent the transmission properties of a system and to characterize the information-bearing attributes of a signal. The best representation for the other purpose. For example the Fourier analysis has had great application in characterizing the transmission properties of linear time invariant systems.

Yet such an analysis is not necessarily the best procedure to specify the information-bearing attributes of a signal. The Fourier resolution is analytically complete and may have infinite dimensionality. However, the best representation of the information-bearing attributes of a signal will be that which has the lowest possible number of dimension, and is therefore, necessarily approximate.

In characterizing the information content of a signal the problem arises in selecting those parameters which lead to the best representation of the signal. Only when these parameters are the amplitudes of the spectral decomposition of the signal is there a linear relationship between the parameters and the signal waveform. Usually, however, the significant parameters are the natural frequencies of the dynamical system, which are non-linearly related to the signal waveform. It is therefore quite difficult to perform mathematical operations on the signal waveform in order to estimate the value of the parameters. Huggins emphasizes that while the precise analytical solution for these parameters may be extremely difficult, experimental attempts at solution should not be discouraged. Such an empirical approach may be inexact in any mathematical sense but may yield a representation which is qualitatively valid and quantitatively useful.



## SIGNAL REPRESENTATION BY DAMPED EXPONENTIALS

The Fourier frequency decomposition of a signal represents one resolution into orthogonal components. Many other complete sets of orthogonal components may be devised for approximating a given signal.

For the class of signals which are characterized temporally by the epochs and intensities of the forcing function and structurally by the transmission properties of the dynamical system, an appropriate representation should portray independently and explicitly both the temporal and structural attributes of the signal. Such a representation can be formulated by the convolution of an impulsive forcing function  $f(t)$  and a system-memory function  $h(\tau)$ .

$$s(t) = f(t) * h(\tau)$$

The temporal attributes of the signal are determined largely by epochs and intensities of the impulsive forcing function whereas the structural characteristics of the signal are primarily determined by the system-memory function.

For convenience sake let  $f(t)$  be an impulsive function with a signal epoch at  $t = 0$ . Then for  $t > 0$ , the signal is represented by  $h(t)$ . The signal can now be characterized by the amplitudes  $A_k$  and the natural frequencies,  $s_k$  of  $h(\tau)$  where

$$h(\tau) = \sum_k A_k e^{s_k \tau} \quad \tau > 0$$

As noted before, however, it is quite difficult to calculate these parameters, especially  $s_k$ , the natural frequencies. Another approach involves approximating  $h(t)$  by a set of coefficients  $B_k$  which are the amplitudes of a linear combination of exponentials whose complex frequencies  $p_k$  are a prescribed set, so that

$$h(t) = \sum_k B_k e^{p_k t}$$

The new set of complex frequencies  $p_k$  are an approximation to the set of natural frequencies  $s_k$ . It is interesting to note that a collection of highly damped exponentials exhibit a strong correlation with one another. For instance, the correlation coefficient between the two damped exponentials  $e^{p_i t}$  and  $e^{p_n t}$  is

$$V_{jn} = \frac{[(p_i + \bar{p}_i)(p_n + \bar{p}_n)]^{1/2}}{p_i + p_n^*}$$

Thus, for example, the exponential  $e^{-15t}$  may be approximated with great accuracy by a combination of  $e^{-1t}$  and  $e^{-2t}$ . It can therefore be appreciated that a preselected set of complex frequencies which "span" a region in the left half of the "s plane" might reasonably represent any complex frequency which fall in the same area.

THE PROBLEM OF SELECTING A BASIS SET

As mentioned in the previous section, one can more or less approximate a signal by a prescribed set of frequencies which "span" a region of the "s plane" wherein

the natural frequencies lie. A difficult problem is encountered, however, in selecting an optimal basis set which minimizes the error between the signal and its representation.

A complete representation for the set of exponentials  $e^{p_k t}$  may be formed by employing Szasz's theorem (10) which states that such a set is complete when and only when

$$\lim_{N \rightarrow \infty} \sum_{k=1}^N \frac{-\operatorname{Re}(p_k)}{1 + |p_k + \frac{1}{2}|^2} = \infty$$

For example, the infinite set  $e^{-t}$ ,  $e^{-2t}$ ,  $e^{-3t}$  ... is a complete set. In fact one could select an unlimited number of complete representations of the signal which involve infinite sets of exponentials. This of course is not a practical approach to the problem. Another approach to the problem involves determining a finite set of N components which, in some manner, is chosen to minimize the mean-square error over the entire ensemble of signals. Such a method has not been adequately solved, although Huggins (8) suspects that there exists an optimum basis set for every specified value of N.

In the absence of a well defined mathematical solution to the problem of choosing a basis set, an empirical selection of components has been used in this investigation. The empirical approach will be presented in a later section.

## CONSTRUCTION OF AN ORTHONORMAL SET OF FUNCTIONS

Assuming that the problem of selecting the set of  $N$  component exponentials has been solved (i.e.  $p_k$  are given), the coordinates  $B_k$  appearing in the representation of  $h(\tau) \doteq \sum_{k=1}^N B_k e^{p_k \tau}$  may be obtained. As noted previously, however, the set of damped exponentials are not uncorrelated and, hence, a change in the amplitude of one component may be more or less neutralized by suitable changes in the amplitudes of the other components (9). This results in mathematical equations whose solutions are excessively sensitive to slight numerical errors.

To avoid this difficulty it is necessary to orthogonalize the components of the prescribed set so that the system-memory function  $h(\tau)$  is best approximated by orthogonal functions as

$$h(\tau) \doteq \sum_{k=1}^N c_k \phi_k(\tau)$$

where the  $\phi_k(\tau)$  are orthogonal functions formed from the prescribed set of complex frequencies and the  $c_k$  are the amplitudes which minimize the mean-square error between  $h(\tau)$  and  $\sum_{k=1}^N c_k \phi_k(\tau)$ .

A unique and simple method to construct orthonormal functions from a prescribed set of component exponentials is contributed by Kautz (11). Given a set of exponential functions  $e^{-s_1 \tau}$ ,  $e^{-s_2 \tau}$ , ...,  $e^{-s_n \tau}$  extending over the semi-infinite interval,  $\tau \geq 0$ ; a set of orthonormal

functions  $\Phi_1(\tau), \Phi_2(\tau), \dots, \Phi_n(\tau)$  may be constructed having frequency-domain representatives as follows:

$$\Phi_1(s) = \frac{\sqrt{-s_1 - \bar{s}_1} \cdot 1}{(s - s_1)}$$

$$\Phi_2(s) = \frac{\sqrt{-s_2 - \bar{s}_2} (s + \bar{s}_1)}{(s - s_1)(s - s_2)}$$

$$\Phi_n(s) = \frac{\sqrt{-s_n - \bar{s}_n} (s + \bar{s}_1)(s + \bar{s}_2) \dots (s + \bar{s}_{n-1})}{(s - s_1)(s - s_2) \dots (s - s_{n-1})(s - s_n)}$$

The orthogonality can be demonstrated in the frequency domain by showing that pole and zero cancellation leads to an inner product,

$$\int_{c-j\omega}^{c+j\omega} \Phi_j(-s) \Phi_k(s) \frac{ds}{2\pi j}$$

in which the integrand is analytic in a half plane when  $j \neq k$  and hence the integral vanishes by Cauchy's integral theorem (12).

If the set of natural frequencies have complex components the equations above yield orthonormal functions which are themselves complex. To obtain real functions from complex exponential components of the form  $s_k = -\alpha + j\omega$ ,  $\bar{s}_k = -\alpha - j\omega$ , the complex conjugates must be added in pairs. As described by Kautz (11) the method is similar except that when the pair of conjugate poles  $s_k$  and  $\bar{s}_k$  are first introduced, a real zero at  $-|s_k|$  is also included along with the two new poles to obtain the first function. For the second function the zero is mirrored on the  $j\omega$  axis at  $+|s_k|$ . For example, given  $s_1, s_2$  and  $s_3$  where  $s_1$

is real and  $S_2$  and  $S_3$  are complex conjugates, the frequency representation of the orthonormal functions is

$$\begin{aligned} \bar{\Phi}_1(s) &= \frac{\sqrt{-s_1 - \bar{s}_1} \cdot 1}{(s - s_1)} \\ \bar{\Phi}_2(s) &= \frac{\sqrt{-s_2 - \bar{s}_2} (s + \bar{s}_1)(s + |s_2|)}{(s - s_1)(s - s_2)(s - s_3)} \\ \bar{\Phi}_3(s) &= \frac{\sqrt{-s_3 - \bar{s}_3} (s + \bar{s}_1)(s - |s_3|)}{(s - s_1)(s - s_2)(s - s_3)} \end{aligned}$$

Kautz' method thus provides a method for constructing a set of orthonormal functions from the prescribed set of exponential components.

### DETERMINATION OF THE SIGNAL COORDINATES

Returning to the problem of specifying  $h(\tau)$  given a set of component exponentials which have been orthogonalized, one may then attempt to solve for the amplitudes of these orthonormal functions which will best approximate  $h(\tau)$ ,

$$h(\tau) = \sum_{k=1}^N c_k \Phi_k(\tau)$$

The amplitudes  $c_k$  will be selected to minimize the mean-square error which is given by

$$E = \int_0^{\infty} [h(\tau) - \sum_{k=1}^N c_k \Phi_k(\tau)]^2 d\tau$$

By setting  $dE/dc_k = 0$  for each  $c_k$  the problem reduces to evaluating the integrals

$$c_k = \int_0^{\infty} h(\tau) \Phi_k(\tau) d\tau \quad k = 1, 2, 3.$$

The solution of the above integral for each  $c_k$  yields a

unique set of coefficients which results in the least mean-square error approximation to  $h(\tau)$ . These coefficients are the coordinates which determine the signal representation.

#### EXPERIMENTAL SELECTION OF COMPONENT EXPONENTIALS

The experimental analysis employed in this paper is limited to the descending portion of the brachial pressure wave because an estimation of the natural frequencies of the waveform has been contributed by Goldwyn and Watt (7). They presented an electrical model (Figure 2) of the arterial system which accounts for the descending segment of the waveform. From this model they derived an unforced system equation, the general solution of which is

$$v_1(t) = \alpha_2 e^{-\alpha_3 t} + \alpha_4 e^{-\alpha_5 t} \cos(\alpha_6 t - \alpha_7)$$

where  $\alpha_3$ ,  $\alpha_5$ , and  $\alpha_6$  are parameters related to  $C_1$ ,  $C_2$ , and  $L$  whereas  $\alpha_2$ ,  $\alpha_4$ , and  $\alpha_7$  are functions of the initial conditions. Based upon the above equation and given a measured brachial pressure curve  $p(t)$ , a digital computer was programmed to determine the set of  $\alpha_i$  so that a least squares approximation of the form

$$p(t) - \alpha_1 = \alpha_2 e^{-\alpha_3 t} + \alpha_4 e^{-\alpha_5 t} \cos(\alpha_6 t - \alpha_7)$$

could be achieved ( $\alpha_1$  is the constant "reference pressure"). The measured pressure curves  $p(t)$  are shown in Figure 3 and the corresponding sets of  $\alpha_i$  are given in Table I.

Note that the natural frequencies, which are the poles of the transfer function, are located on the "s plane" at  $-\alpha_3$  and  $-\alpha_5 + j\alpha_6$ . For the "normal" patient these values are  $-3.68$  and  $-4.07 \pm j23.6$  respectively (Figure 4).

Admittedly these values represent only the natural frequencies from one normal patient. However, given the difficulties in finding an optimal basis set as mentioned earlier in the paper, it was decided to use these parameters in an empirical approach to the problem of selecting the basis set. Thus the component exponentials employed in this analysis consist of  $e^{-3.68\tau}$ ,  $e^{-(4.07+j23.6)\tau}$  and  $e^{-(4.07-j23.6)\tau}$ .

#### CONSTRUCTION OF THE EXPERIMENTAL SET OF ORTHONORMAL FUNCTIONS

Utilizing Kautz's procedure we can now form the orthonormal functions from the set of exponents described above. The dominant component appears to be  $e^{-3.86\tau}$  which we have selected to be the fundamental component  $s_1$ , from which  $\Phi_1(\tau)$  is formed, viz,

$$\Phi_1(s) = \frac{\sqrt{7.72} \cdot 1}{(s + 3.86)}$$

$$\Phi_1(\tau) = \mathcal{L}^{-1}[\Phi_1(s)] = \sqrt{7.72} e^{-3.86\tau}$$

If  $s_2$  and  $s_3$  are the complex conjugates  $-4.07 \pm j23.6$ , then



$\Phi_2(\tau)$  &  $\Phi_3(\tau)$  are formed in a similar manner

$$\Phi_2(s) = \frac{\sqrt{8.14} (s-3.86)(s+24)}{(s+3.86)(s+4.07-j23.6)(s+4.07+j23.6)}$$

$$\Phi_2(\tau) = \sqrt{8.14} (-.277 e^{-3.86\tau} + 1.39 e^{-4.07\tau} \cos(23.6\tau - 22^\circ))$$

$$\Phi_3(s) = \frac{\sqrt{8.14} (s-3.86)(s-24)}{(s+3.86)(s+4.07-j23.6)(s+4.07+j23.6)}$$

$$\Phi_3(\tau) = \sqrt{8.14} (.386 e^{-3.86\tau} + 1.64 e^{-4.07\tau} \cos(23.6\tau + 68^\circ))$$

These three orthonormal functions  $\Phi_1(\tau)$ ,  $\Phi_2(\tau)$  and  $\Phi_3(\tau)$  are the basis functions which were used in analyzing the pulse waves.

To prove that these functions were in fact orthonormal a computer performed the following operations over 1.2 seconds.

$$\int \Phi_1(\tau) \Phi_1(\tau) d\tau = .999$$

$$\int \Phi_2(\tau) \Phi_2(\tau) d\tau = .994$$

$$\int \Phi_3(\tau) \Phi_3(\tau) d\tau = .992$$

$$\int \Phi_1(\tau) \Phi_2(\tau) d\tau = .015$$

$$\int \Phi_1(\tau) \Phi_3(\tau) d\tau = .007$$

$$\int \Phi_2(\tau) \Phi_3(\tau) d\tau = .005$$

These results correlate well with the requirement for orthonormal functions which is

$$(\Phi_j(\tau), \Phi_k(\tau)) = \int_0^{\infty} \Phi_j(\tau) \Phi_k(\tau) d\tau = \begin{cases} 1, & j=k \\ 0, & j \neq k \end{cases}$$

## DATA AND METHODS

Twenty-five pressure curves, shown in Figure 5, were obtained from a study by Hancock and Abelmann (13). The curves are direct brachial arterial pressure tracings obtained by insertion through the skin of an 18 gauge needle into the brachial artery at the crook of the arm. The needle was connected by a rigid tubing to an electro-manometer and the tracing was recorded on a direct-writing oscillograph.

Of the twenty-five patients, ten were "normal subjects" whose age ranged from 20 to 37 years old. Seven patients had proved severe aortic stenosis (narrowing of the valvular aperture). Three patients had proved severe aortic stenosis in combination with aortic regurgitation (incompetent aortic valve). Three patients had pure aortic regurgitation and two patients had mitral insufficiency (incompetent valve between left ventricle and left atrium).

The three pressure tracings contributed from the work of Goldwyn and Watt (7) were also included in the analysis. One patient was normal, one had aortic regurgitation, and the third had a cardiomyopathy.

The descending limb of the twenty-eight pressure curves are normalized in the following manner. The "d-c" or end-diastolic pressure was then subtracted from the curve so that each curve decayed to "zero". Each tracing was then

normalized in magnitude by dividing each pressure point on the curve by the highest pressure value. The normalized curves were then sampled at 40 milleseconds. A digital computer reconstructed the pressure tracings from the sampled points by a second order approximation method. The computed pressure tracings were the  $h(\tau)$  used in the experimental analysis. It is realized that perhaps information is lost in such a normalizing procedure. On the other hand we are primarily concerned here with waveform analysis and not with magnitude analysis.

Given the waveforms  $h(\tau)$  and the orthonormal functions  $\phi_k(\tau)$ , a digital computer was programmed to calculate the signal coordinates  $c_k$  from the integral

$$c_k = \int_0^{\infty} h(\tau) \phi_k(\tau) d\tau \quad k=1,2,3$$

The error of the approximation,  $h(\tau) \approx \sum_{k=1}^3 c_k \phi_k(\tau)$ , was evaluated by two methods. The error function  $\epsilon(\tau)$  defined by

$$\epsilon(\tau) = h(\tau) - \sum_{k=1}^3 c_k \phi_k(\tau)$$

was plotted by the computer along with its respective waveforms  $h(\tau)$  and its approximation  $\sum_{k=1}^3 c_k \phi_k(\tau)$ . The second method involved calculating the integral of the squared error, viz,

$$E = \int_0^{\infty} \left[ h(\tau) - \sum_{k=1}^3 c_k \phi_k(\tau) \right]^2 d\tau$$

## RESULTS AND DISCUSSION

The calculated signal coordinates for the twenty-eight waveforms, together with each patient's diagnosis, are listed in Table II. The ranges of the  $c_k$  for normal patients are:  $.28 < c_1 < .46$ ,  $-.031 < c_2 < .075$ , and  $-.033 < c_3 < .026$ . The ranges for abnormal patients are:  $.22 < c_1 < .37$ ,  $-.006 < c_2 < .083$ , and  $-.043 < c_3 < .061$ . The relationship between  $c_1$ , the pure exponential component, and  $c_2$ , the largest damped sinusoidal component, is plotted in Figures 6, 7, and 8. Figure 6 shows the plotted points in both normal and abnormal patients. Figures 7 and 8 are graphs showing the same points separated into normal and abnormal patient categories. In general the abnormal group, especially those with combined aortic stenosis and regurgitation, tend to have a lower  $c_1$  component and a higher  $c_2$  component than the normal group. While the signal coordinates themselves do not provide an absolute separation of abnormal from normal patients, these parameters quantify arterial waveforms and should be useful in measuring the effect of stress, drugs, etc., at least in individual patients.

The magnitude of the "a-c" component of the signal is considered in Figures 9 and 10 which are histograms showing the relationship of this magnitude to normal and abnormal patients respectively. Note that the abnormal

patients tended to have a greater "a-c" component than normal patients. It should be noted, however, that the abnormal group is also older than the normal group. One may postulate that the more elastic arterial system in the younger group may filter the "a-c" components which are observed in the older group.

Figures 11-20 are plots from individual patients. In each figure the upper plot consists of two functions:  $h(\tau)$ , the normalized brachial waveform (cross hatched line), and  $\sum_{k=1}^3 c_k \phi_k(\tau)$  which is the best approximation to  $h(\tau)$ . The lower plot in each figure represents the error function  $E(\tau)$ , which has been normalized so that the maximum positive error is one. The true maximum positive error and the integral of the squared error,  $E$ , is indicated in the upper right hand portion of the figure. The integral of the squared error is also given in Table III for each patient. The value of the integral of the squared error did not appear to differentiate normal from abnormal patients. Note that the error function  $E(\tau)$  represents the remainder of  $h(\tau)$ . Hence,  $E(\tau)$  is orthogonal to the component functions  $\phi_1(\tau)$ ,  $\phi_2(\tau)$ , and  $\phi_3(\tau)$ . i.e.

$$\int_0^1 E(\tau) \phi_k(\tau) d\tau = 0 \quad k=1,2,3$$

In the limited number of cases observed, similar patterns of  $E(\tau)$  were observed in certain abnormal patients.

## SUMMARY OF RESULTS

1. The group of patients with cardiac valvular disease tended to have a greater "a-c" component in their pressure waveforms than the group of young normals.
2. The waveform of the error function was observed to be similar in certain abnormal patients.

## SUGGESTIONS FOR FURTHER STUDY

1. Investigation of the error function to ascertain whether "abnormal" information is contained in the waveform.
2. Extension of the exponential analysis to include the ascending limb of the arterial pulse wave.
3. The use of exponential analysis to screen large numbers of patients for the presence of heart disease and/or peripheral vascular disease.

TABLE I  
 Computed Parameters  $\alpha_i$  For Selected Patients  
 (from Goldwyn and Watt)

Patient	26	27	28
Clinical Status*	N	CM	AR
$\alpha_1$	68.5	38.9	41.5
$\alpha_2$	68.9	47.8	140.5
$\alpha_3$	3.86	3.06	7.01
$\alpha_4$	-13.2	21.7	-21.6
$\alpha_5$	4.07	2.74	3.27
$\alpha_6$	23.6	22.6	19.8
$\alpha_7$	-1.73	0.54	-1.32

\*  
 N normal  
 CM cardiomyopathy  
 AR aortic regurgitation

TABLE II

Patient	Clinical Status*	$c_1$	$c_2$	$c_3$
1	N	0.458	-0.031	0.001
2	N	0.291	0.075	-0.002
3	N	0.280	0.025	-0.016
4	N	0.326	0.034	-0.033
5	N	0.327	0.041	-0.002
6	N	0.345	0.020	-0.019
7	N	0.344	0.003	0.007
8	N	0.333	0.053	-0.008
9	N	0.351	-0.000	0.026
10	N	0.402	0.005	-0.030
11	AS & AR	0.221	0.051	0.006
12	AS	0.353	0.027	-0.017
13	AS	0.330	0.012	0.012
14	AS	0.319	0.057	-0.037
15	AS	0.307	0.046	-0.021
16	AS & AR	0.217	0.053	-0.000
17	AS & AR	0.221	0.083	-0.028
18	AS	0.272	0.059	-0.019
19	AS	0.219	0.064	-0.011
20	AS	0.316	0.040	0.003
21	AR	0.272	0.063	-0.043
22	AR	0.348	-0.006	-0.007
23	AR	0.316	0.041	-0.022



TABLE II

Patient	Clinical Status**	$c_1$	$c_2$	$c_3$
24	MR	0.367	-0.003	0.061
25	MR	0.315	0.065	0.014
26	N	0.272	0.033	-0.052
27	CM	0.270	0.107	-0.021
28	AR	0.282	0.082	-0.020

\*  
N normal  
CM cardiomyopathy  
AR aortic regurgitation  
AS aortic stenosis  
MR mitral regurgitation

TABLE III

Patient	Integral of Squared Error	Max. Pos. Error
1	.000544	.159
2	.000255	.121
3	.000297	.189
4	.000416	.085
5	.000257	.066
6	.000303	.107
7	.000354	.150
8	.000666	.227
9	.000335	.099
10	.000408	.109
11	.000282	.209
12	.000659	.103
13	.000135	.070
14	.000286	.071
15	.000366	.098
16	.000485	.239
17	.000886	.214
18	.000562	.122
19	.000718	.229
20	.000322	.073
21	.000585	.176

TABLE III

Patient	Integral of Squared Error	Max. Pos. Error
22	.000156	.071
23	.000171	.057
24	.001616	.200
25	.000190	.099
26	.000398	.086
27	.000237	.052
28	.000652	.292

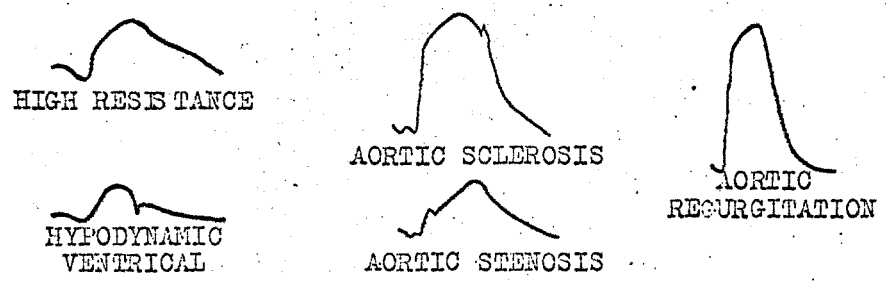


Figure 1. Central arterial waveforms in some common clinical conditions. ( from Wiggers )

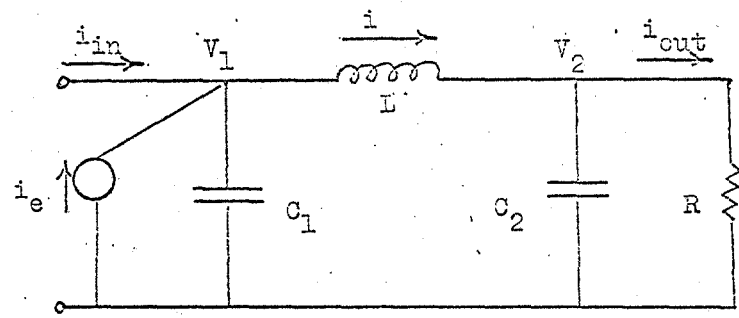


FIGURE 2. In this figure  $v_1$  and  $v_2$  represent the pressures in the central and peripheral vessels respectively. Likewise  $C_1$  and  $C_2$  are related to the elasticity of the arteries. The inductance  $L$  takes into account the inertia of the blood. (from Goldwyn and Watt)

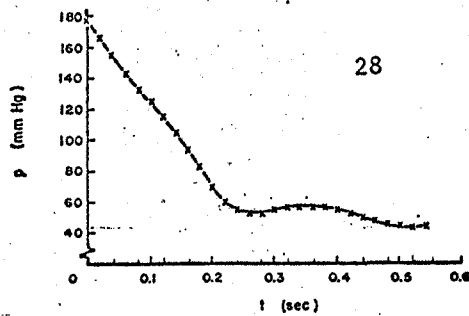
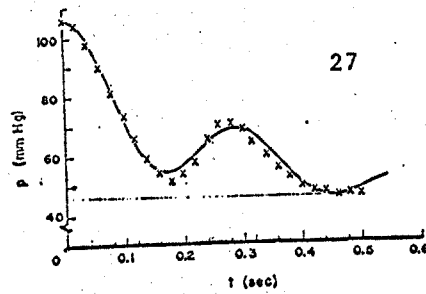
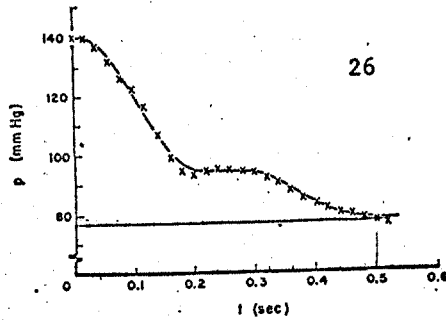
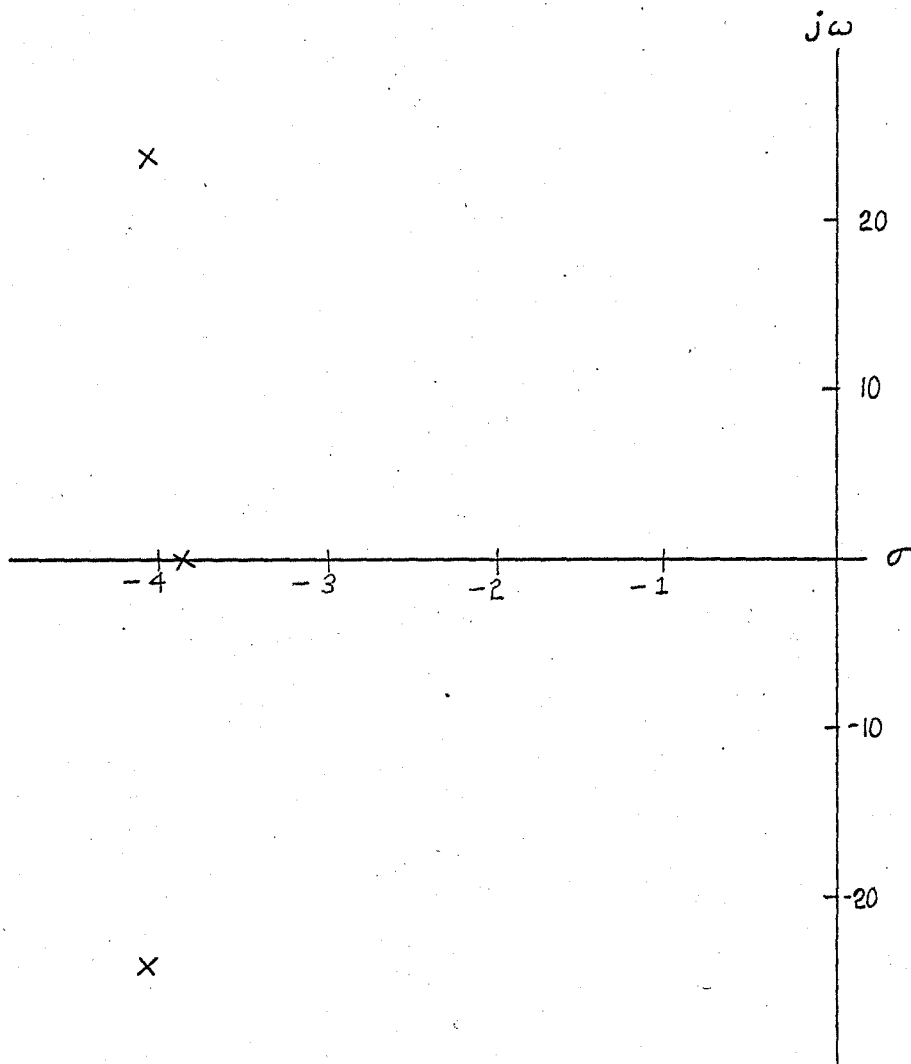


FIGURE 3. The above pulse waveforms are taken from Goldwyn and Watt. From top to bottom, the patients' clinical diagnoses are "normal", cardiomyopathy, and aortic regurgitation.

FIGURE 4



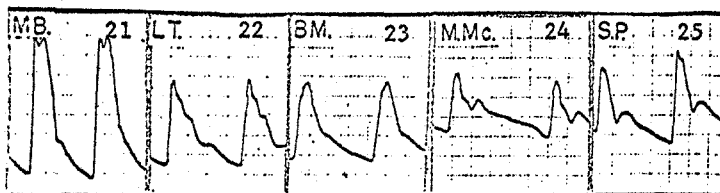
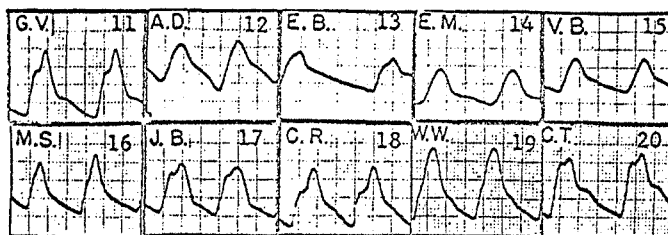
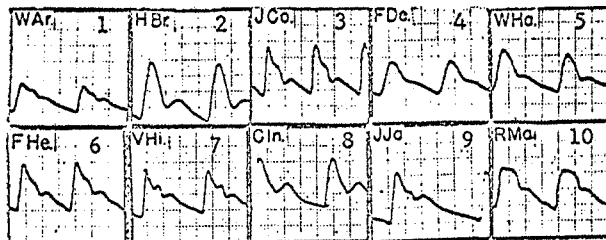


FIGURE 5. The above pulse waveforms are taken from Hancock and Abelmann. The first group are normal subjects. The middle group have severe aortic stenosis. The first three of the lower group have aortic regurgitation while the other two have mitral regurgitation.



FIGURE 6.

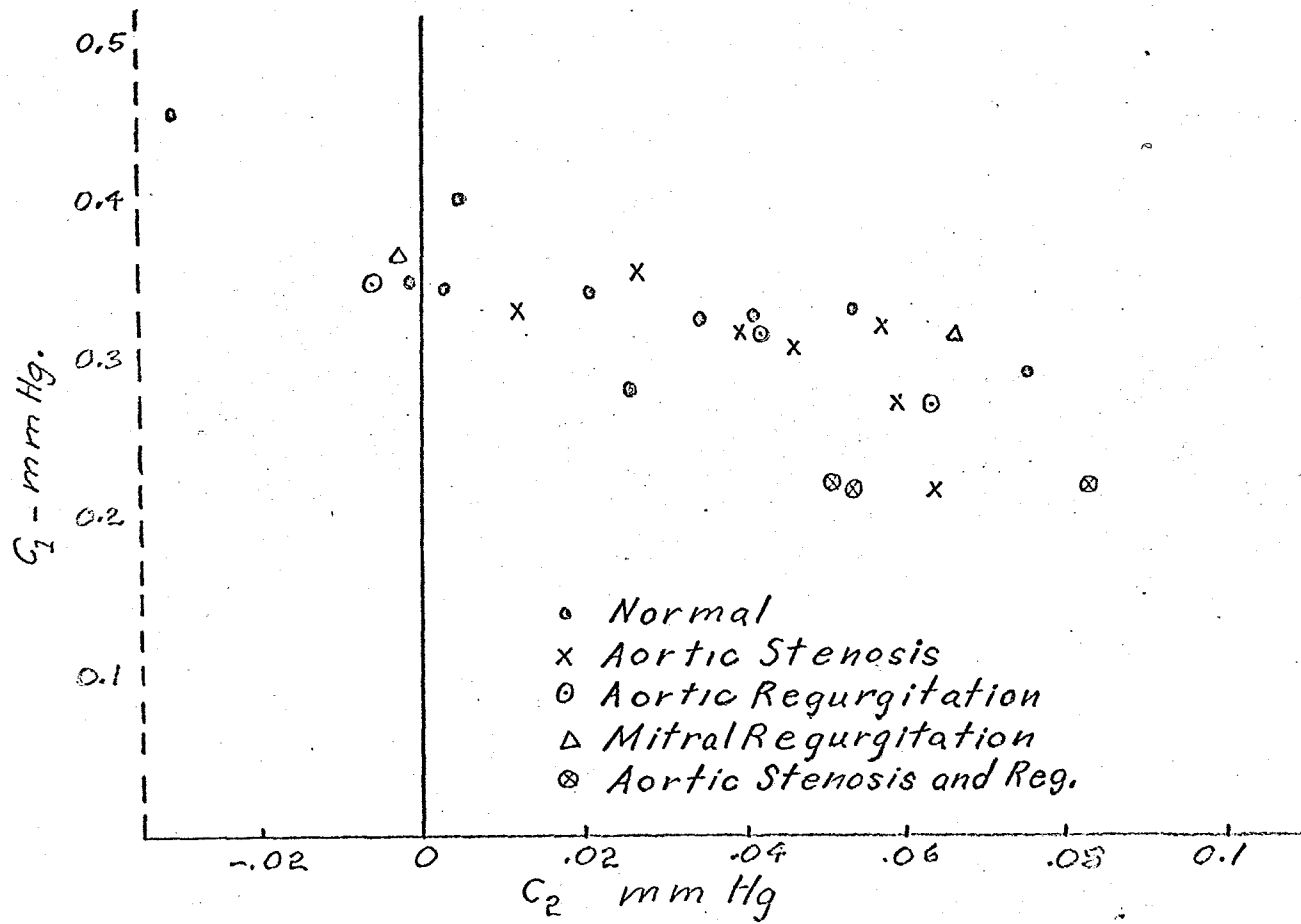


FIGURE 7.

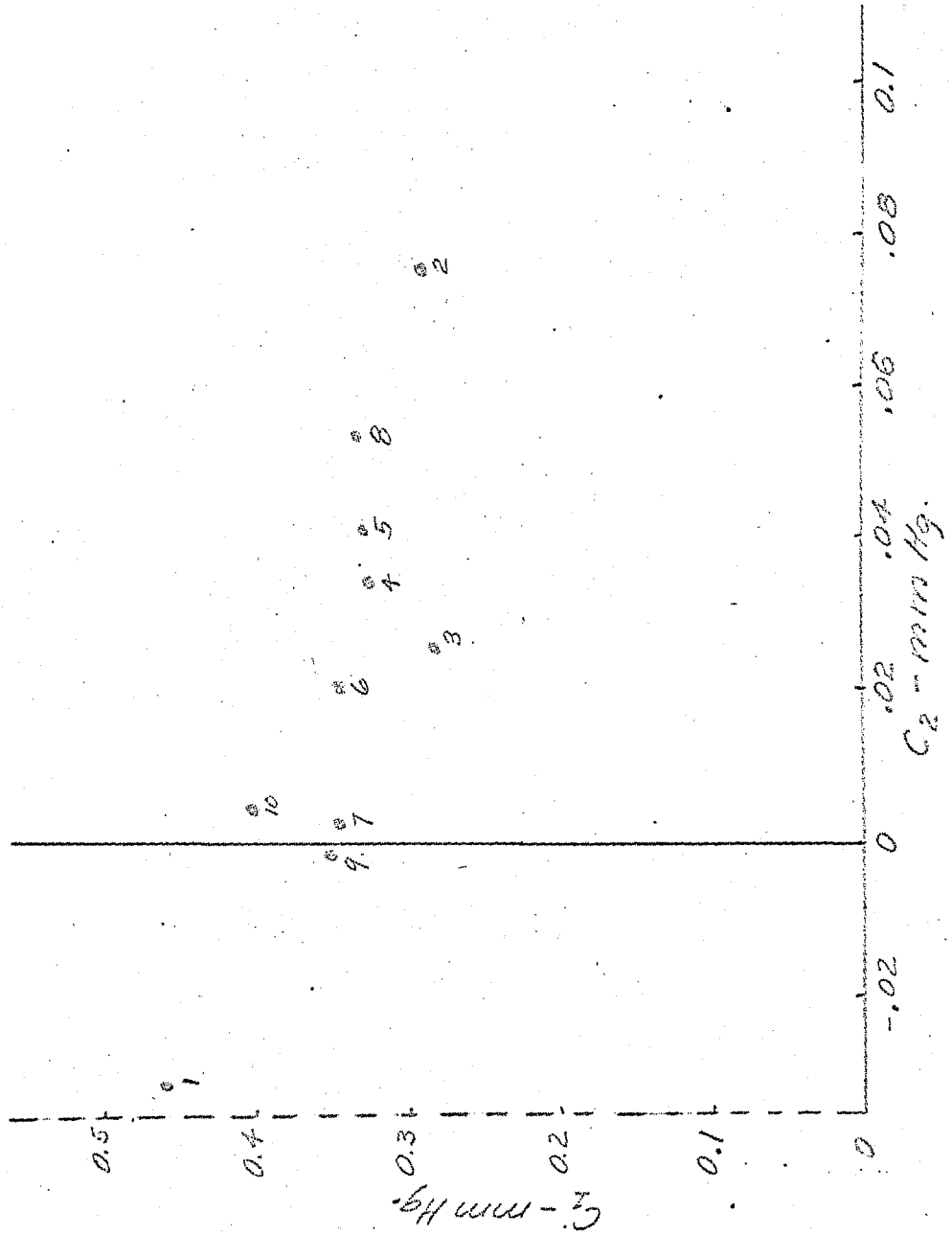


FIGURE 8.

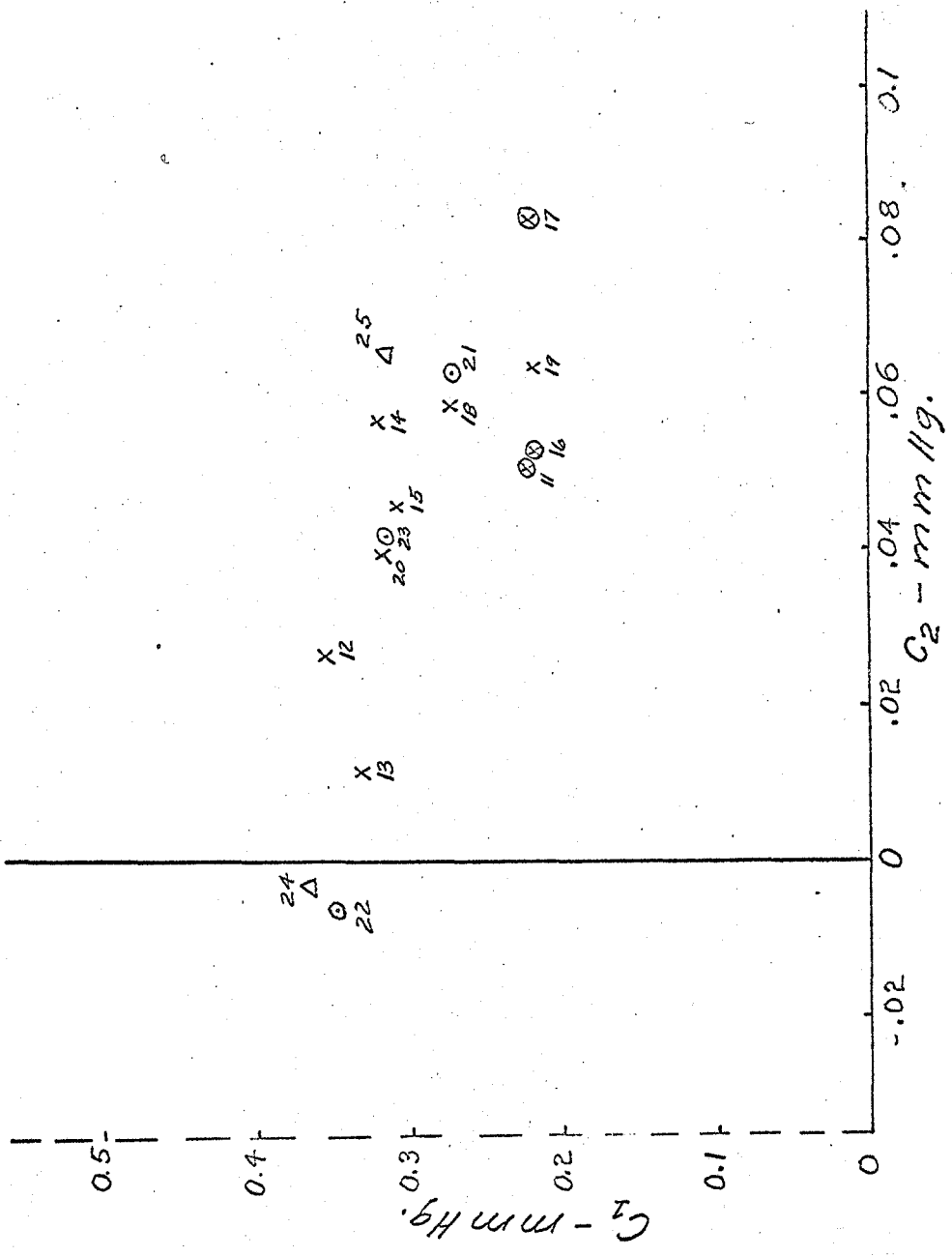


FIGURE 9.

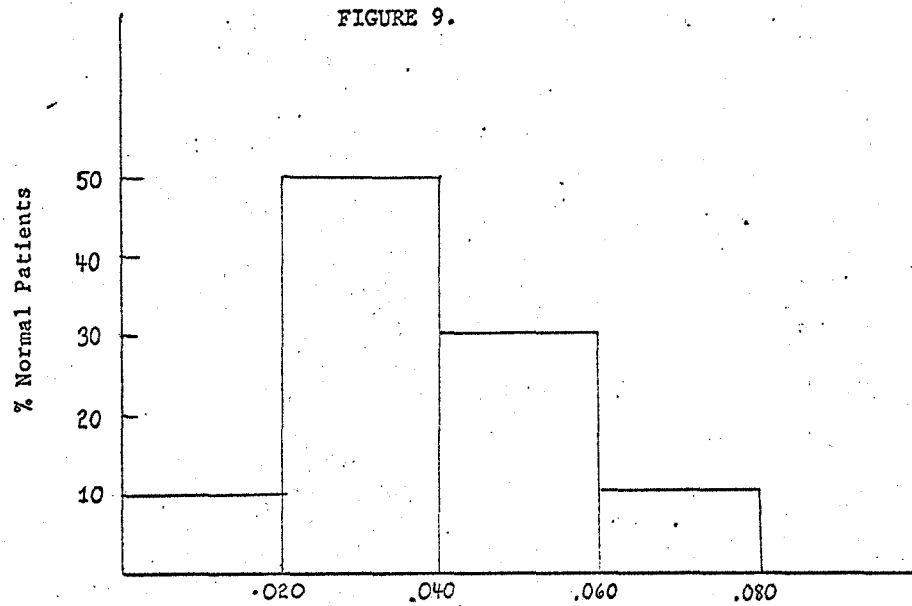


FIGURE 10.

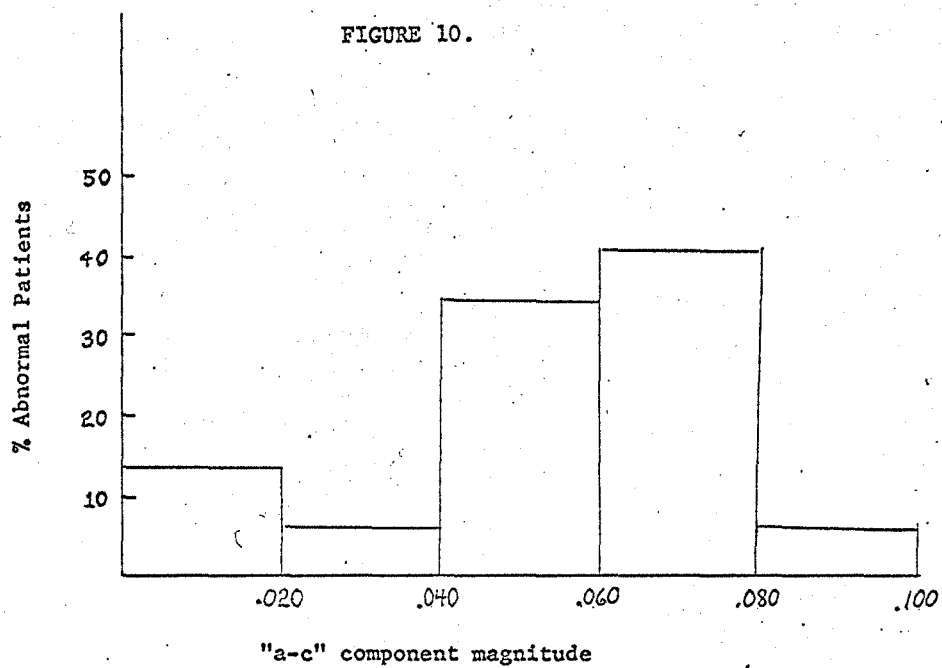


FIGURE 11.

Integral of the squared error = 0.00026

Maximum positive error = .121

Patient 2

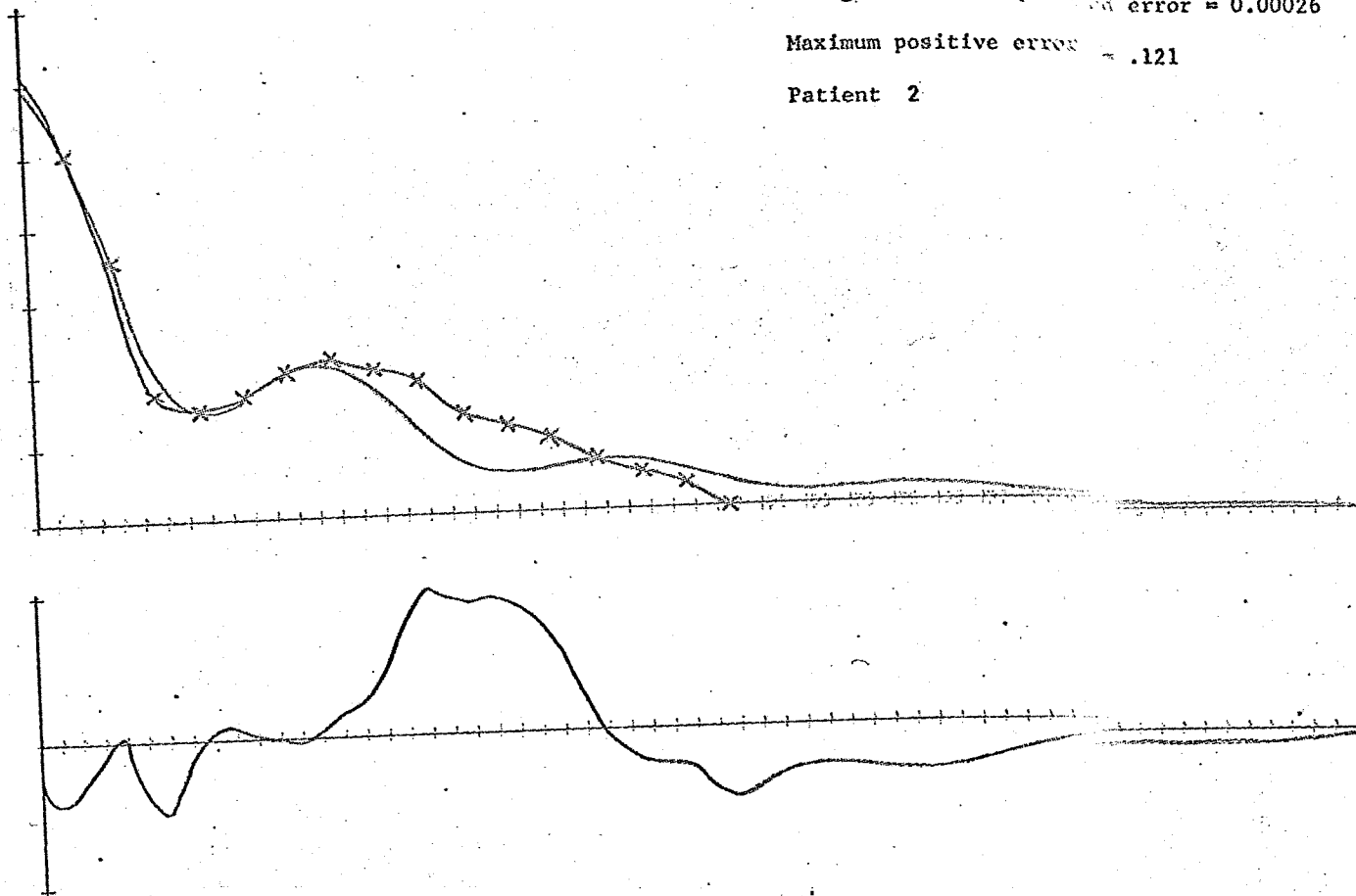


FIGURE 12.

Integral of the squared error = 0.00030

Maximum positive error = .107

Patient 6

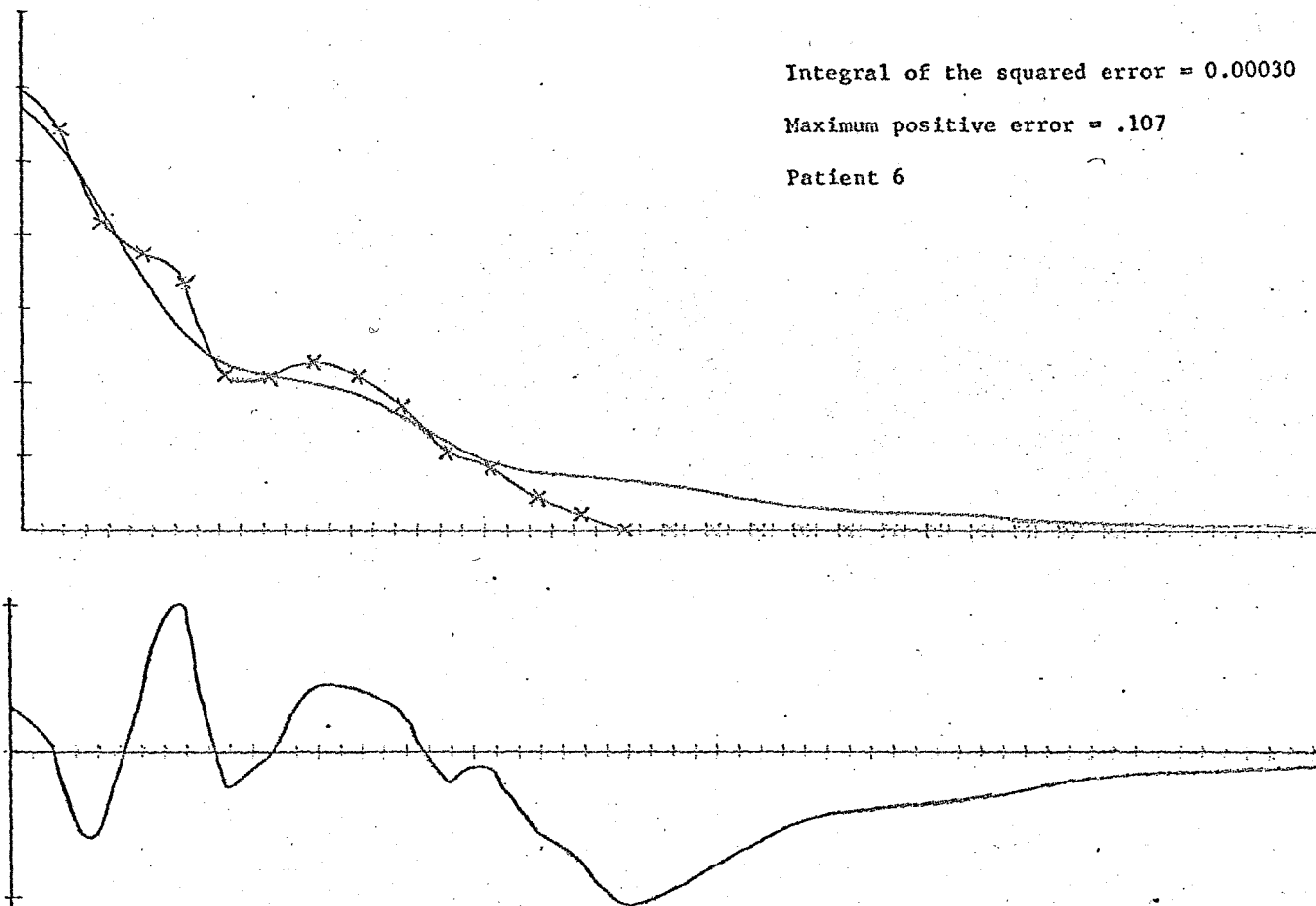


FIGURE 13.

Integral of the squared error = 0.00067

Maximum positive error = .227

Patient 8

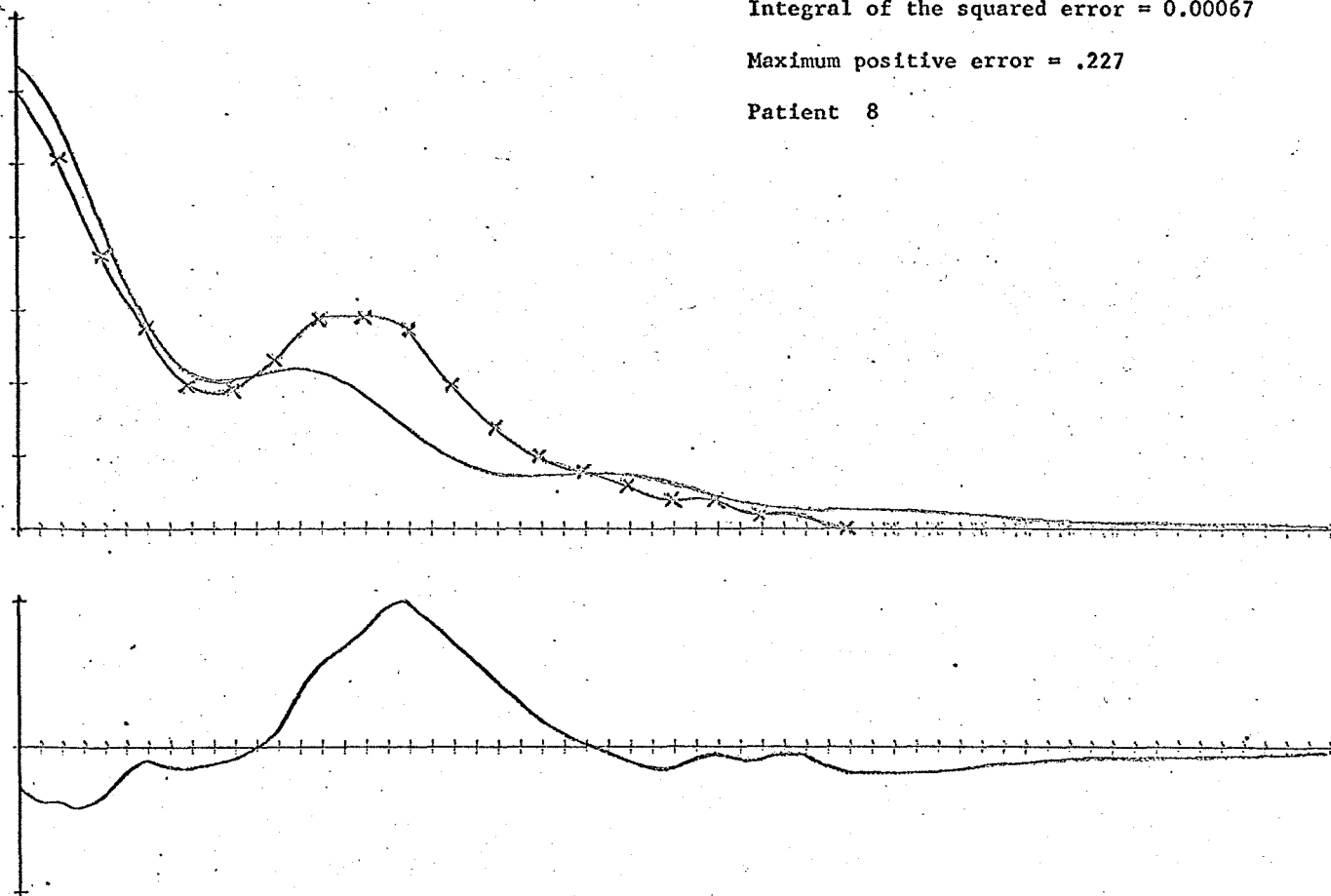


FIGURE 14.

Integral of the squared error = 0.00029

Maximum positive error = .071

Patient 14

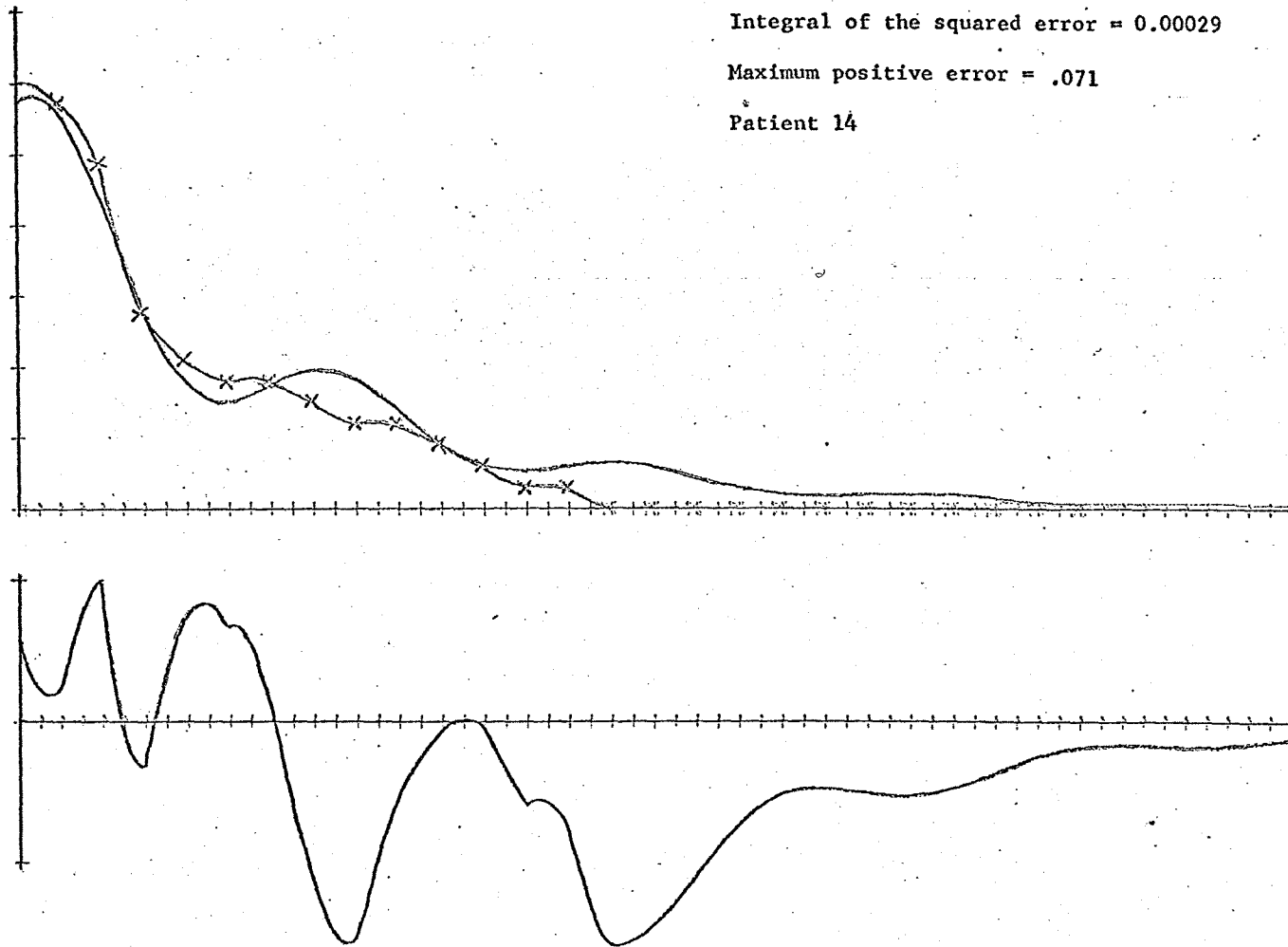




FIGURE 15.

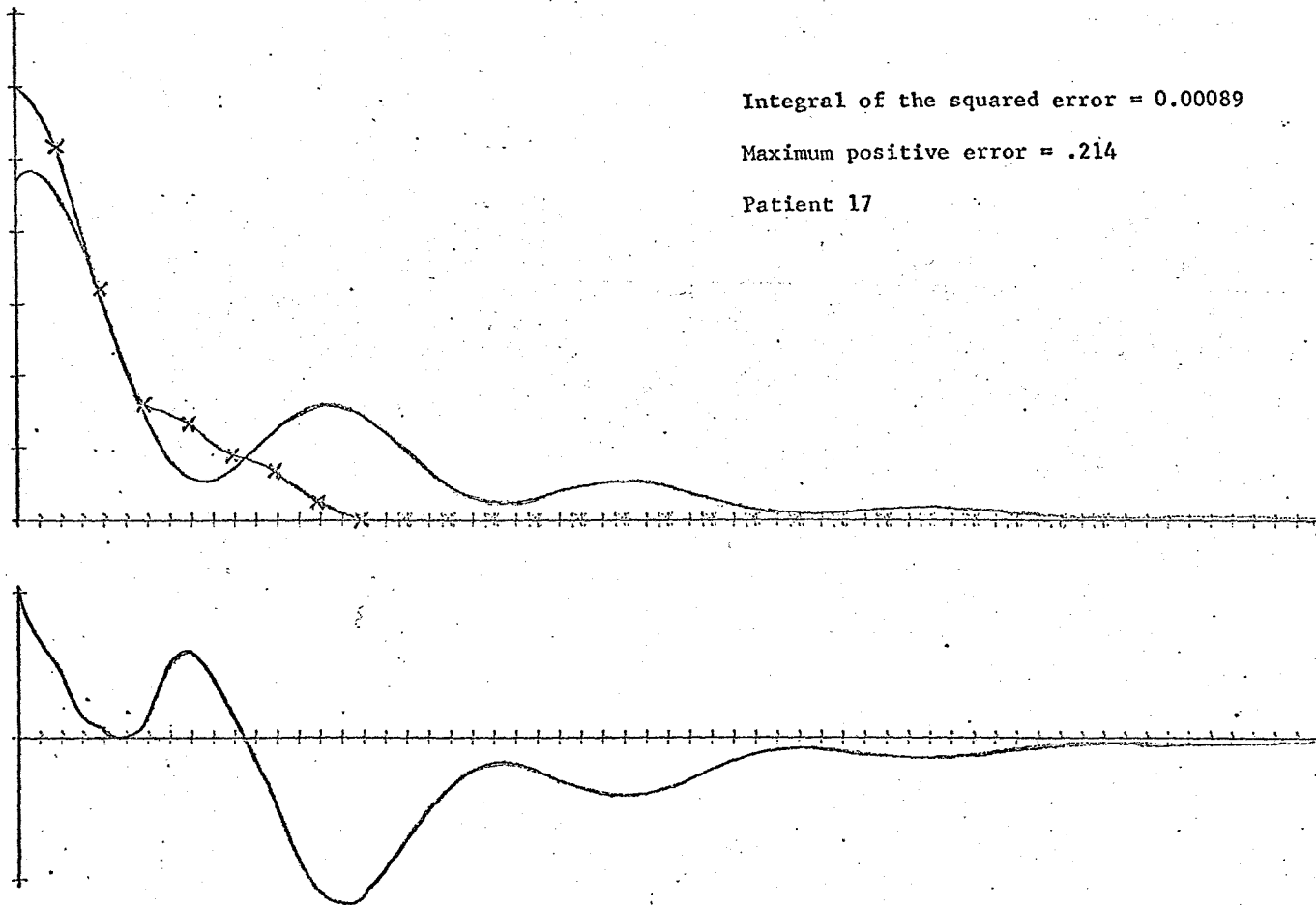


FIGURE 16.

Integral of the squared error = 0.00072

Maximum positive error = .228

Patient 19

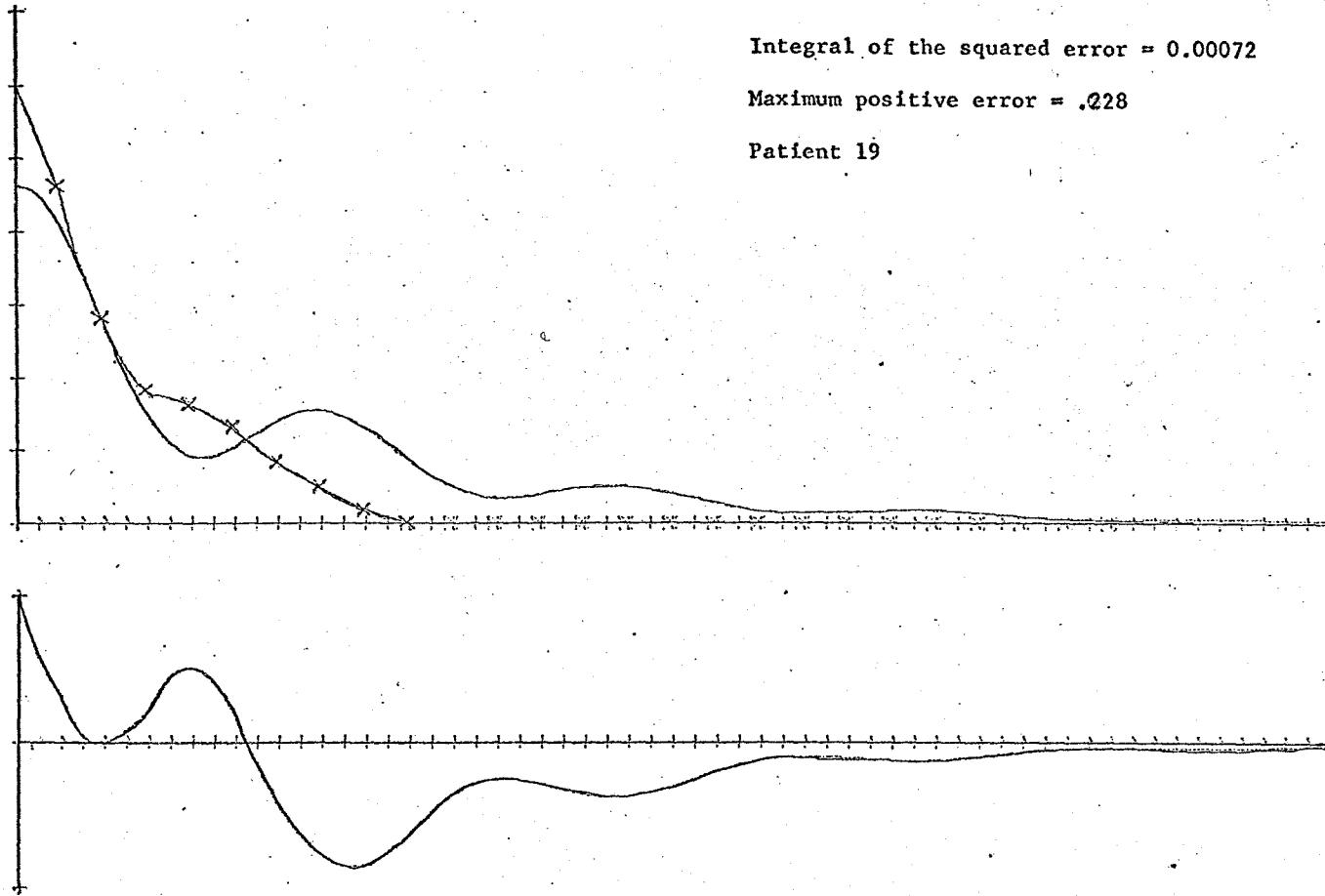


FIGURE 17.

Integral of the squared error = 0.00017

Maximum positive error = .057

Patient 23

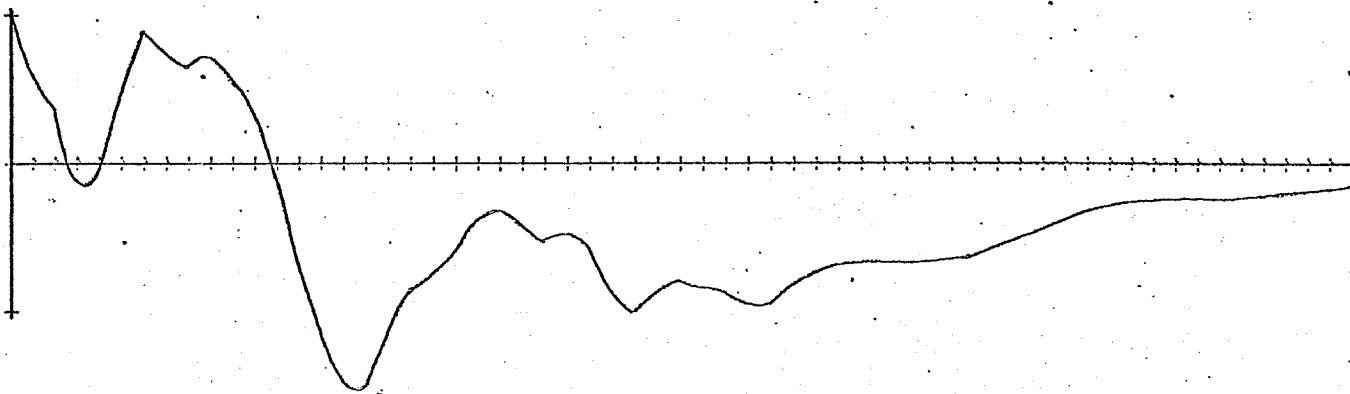
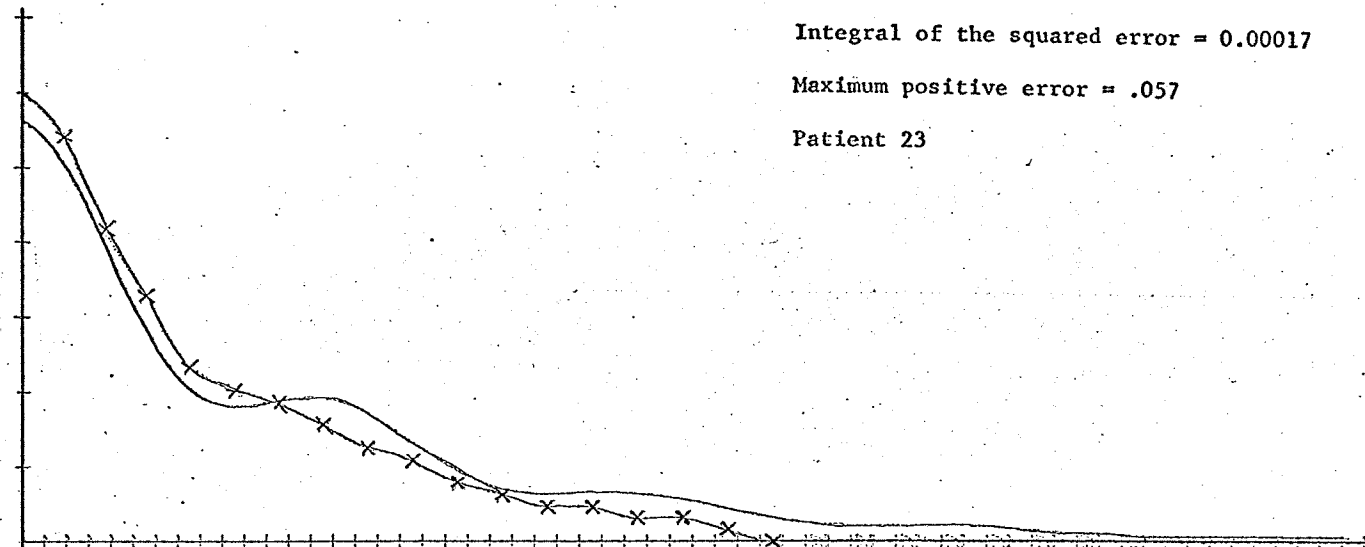


FIGURE 18.

Integral of the squared error = 0.00040

Maximum positive error = .086

Patient 26

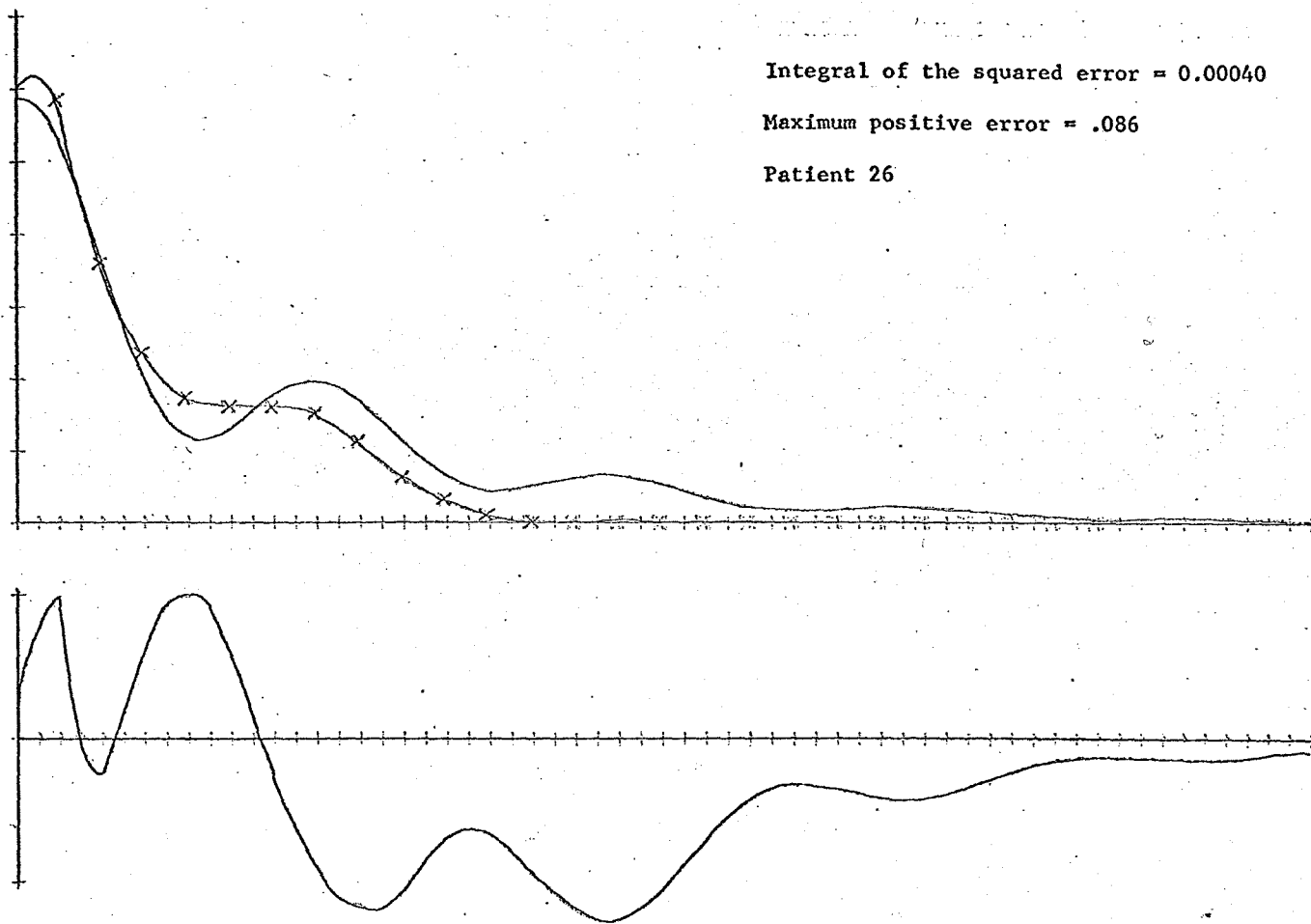


FIGURE 19

Integral of the squared error = 0.00024

Maximum positive error = .052

Patient 27

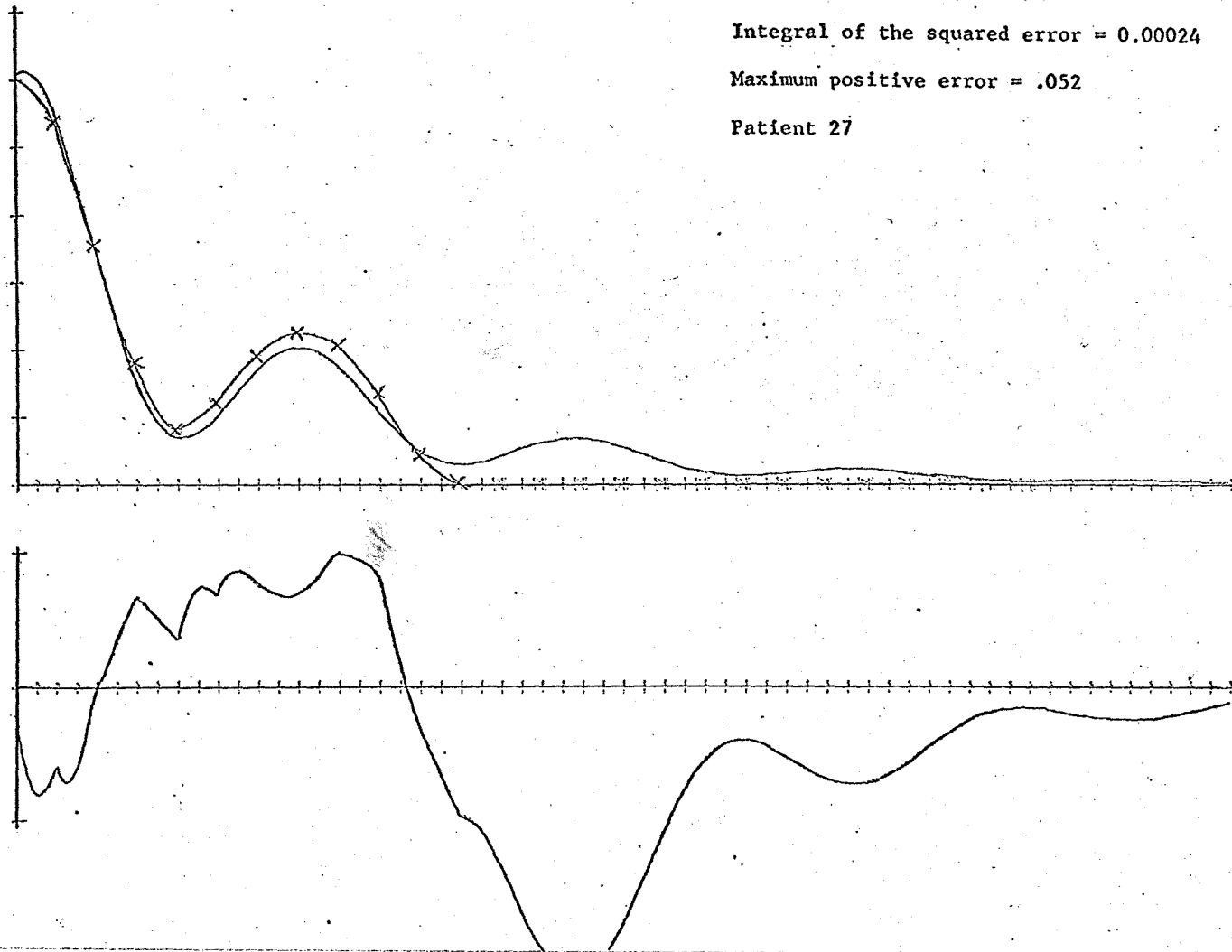
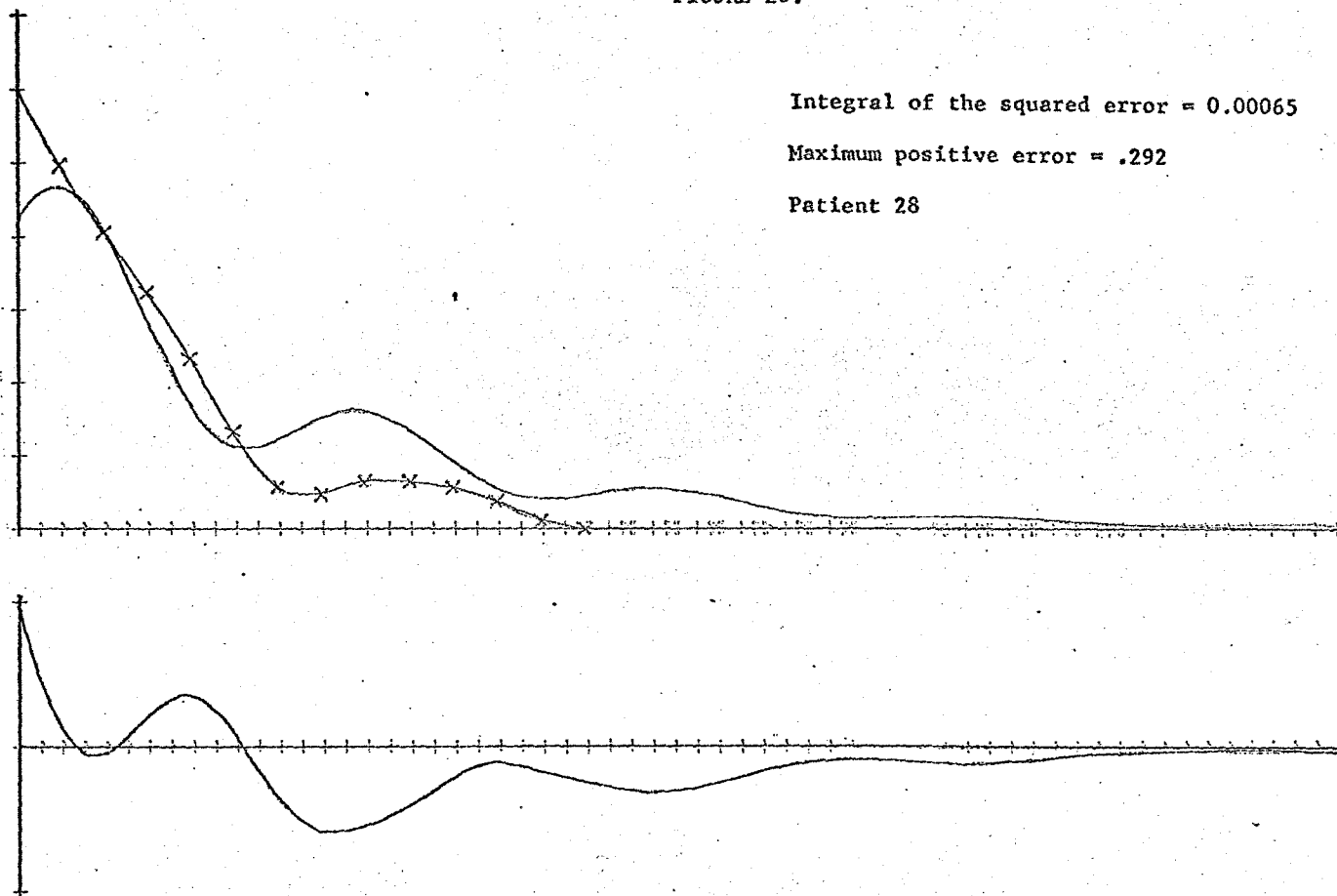


FIGURE 20.

Integral of the squared error = 0.00065

Maximum positive error = .292

Patient 28



## BIBLIOGRAPHY

- 1) DeGowin E.L. Bedside Diagnostic Examination. New York, N.Y., Macmillan, 1965.
- 2) Wiggers C.J. Physiology in Health and Disease. Philadelphia, Penn., Lea and Febiger, 677-680, 1949.
- 3) Mason D.T. Diagnostic Value of the First and Second Derivatives of the Arterial Pressure Pulse in Aortic Valve Disease. Circulation 30: 90-100, 1964.
- 4) Arani D.T., Charleton R.A. Assessment of Aortic Valvular Stenosis from the Aortic Pressure Pulse. Circulation 36: 30-35, Jul. 1967.
- 5) Simmons E.M. A Computer Program for the Peripheral Pulse Wave. Amer. J. Cardiology 19: 827-31, Jun. 1967.
- 6) Puls R., Heizer K. Pulse-Wave Changes With Aging. J. Amer. Ger. Soc. 15 (2): 153-165, Feb. 1967.
- 7) Goldwyn R., Watt T. Arterial Pressure Pulse Contour Analysis via a Mathematical Model for the Clinical Quantification of Human Vascular Properties. IEEE Trans. Bio-Med. Engin. 14 (1): 11-17, Jan. 1967.

- 8) Huggins W.H. Signal Theory. IRE Trans. on Circuit Theory. CT-3 (4): Dec. 1956.
- 9) Huggins W.H. Representation and Analysis of Signals Part I. The Use of Orthogonalized Exponentials. AFRC Report No. TR-57-357, ASTIA Document No. AD 133741: Sept. 30, 1957, Reprinted: Oct. 11, 1963.
- 10) Paley, R.E., Wiener N. Fourier Transforms in the Complex Domain. American Mathematical Society Colloquium Publications, New York, N.Y., XIX; 1934.
- 11) Kautz W.H. Transient Synthesis in the Time Domain. IRE Trans. on Circuit Theory. CT-1 (3): 29-39, Sept. 1954.
- 12) Churchill R.V. Complex Variables and Applications. New York, N.Y., McGraw-Hill, 1960.
- 13) Hancock E.W., Abelmann W.H. A Clinical Study of the Brachial Arterial Pulse Form. 16 (2): 572-581, 1957.